

## LANGERHANS' CELL HISTIOCYTOSIS

**Khomdao BOONCHIT<sup>1</sup>, Jiraporn SRINAKARIN<sup>2</sup>,  
Dumrongsuk BOONCHIT<sup>3</sup>, Warinthorn BUNCHALEAW<sup>4</sup>**

### ABSTRACT

Langerhans' cell histiocytosis, previously called histiocytosis X is an inappropriate proliferation and infiltration of various tissues with cells that are morphologically and immunologically similar to normal Langerhans cells that is probably due to an immune regulatory defect.

We report two different cases of Langerhans' cell histiocytosis. First case is a 1 year 5 months old girl presented with left eye lid swelling and erythema. Second case is a 2 years old girl presented with multiple skull masses and diabetes insipidus.

In 1953, Lichtenstein<sup>1,2</sup> proposed the term histiocytosis X for a group of clinical syndromes of unknown cause characterized morphologically by the proliferation of a unique histiocyte with cytoplasmic inclusions known as X bodies.

In 1980s, it was recognized that the mononuclear cells that populate these lesions were not histiocytes of the usual type, but were in reality a particular cell type: the Langerhans cell<sup>3</sup>. It has pale eosinophilic cytoplasm and a central nucleus with a characteristic groove that differentiates it from other histiocytes. The distinctive feature of

LCH is proliferation of the Langerhans cell, a tissue based histiocyte that is normally found in skin, some mucous membranes, the T zone of lymph nodes, and thymus<sup>4</sup>. Ultrastructurally, the most characteristic feature of the Langerhans cell is the Birberk granule. In addition there are immunologic features of the Langerhans cell that are typical, including S-100 protein positivity, expression of the HLA-DR antigen, and staining with OKT-6 monoclonal antibody<sup>4</sup>. Regardless of clinical presentation, the diagnosis of LCH is based on the identification of Langerhans cell in typical lesions. (table 1)<sup>1,6</sup>

**LCH** = Langerhans' Cell Histiocytosis

**TABLE 1 LANGERHANS' CELL HISTIOCYTOSIS**

Levels of diagnosis

Presumptive

Conventional histopathology

Diagnosis

Immunohistochemistry (S-100 protein)

Enzymatic activity (adenosine triphosphatase,  $\alpha$ -D-mannosidase)

Definitive

Electron microscopy (Birberk granules)

Immunohistochemistry (peanut lectin, OKT-6 antigenicity)

<sup>1</sup> Department of Radiology, Udonthani Hospital, Meung, Udonthani, 41000 Thailand.

<sup>2,4</sup> Department of Radiology, Srinakarind Hospital, Faculty of Medicine, Khon Kaen University, 40002 Thailand.

<sup>3</sup> Department of Plastic and Reconstruction Surgery, Udonthani Hospital, Meung, Udonthani, 41000 Thailand.

There are three well-established clinical subsets of LCH that should be defined at this time: eosinophilic granuloma of bone, Hand-Schuller-Christian disease and Letterer-Siwe disease.

The head and neck region is the most common sites of involvement by LCH.<sup>3</sup> Lesions in children are most commonly located in bone or bone marrow.<sup>5</sup> Orbital involvement of LCH is not uncommon.<sup>6</sup> It has a predilection for young children 1-4 years old.<sup>5</sup> The overall incidence of orbital involvement in a large series of 76 children with LCH was 23%.<sup>2</sup>

**CASE REPORTS**

**CASE 1**

1 year 5 months old girl presented with 2 month history of upper eyelid swelling with

erythema and proptosis of left eye.

On examination, she appeared to be healthy and normally developed. Pupils and extraocular movements were normal. The left eye was slightly proptotic, without ecchymosis surrounding the eye.

Orbital CT SCAN without and with contrast enhancement showed an enhancing fairly well-defined extraconal mass, encroaching lacrimal gland with bony destruction at superolateral aspect of left orbit, involving the greater wing of sphenoid bone. (Fig.1a,b)

An incisional biopsy without curettage was done. Histologic examination was diagnosis for LCH.



**Fig.1a,b** Axial CECT shows enhancing lesion with bony destruction involving the superolateral wall of left orbit

CECT = Contrast Enhancement CT.

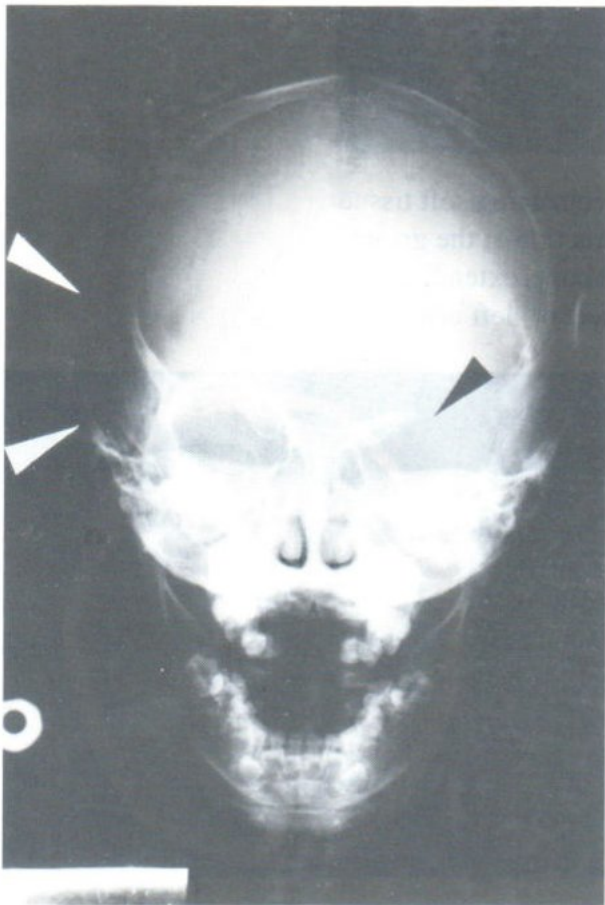
**CASE 2**

2 year-old-girl was admitted to Udonthani hospital in July 1998 with a 4 month history of mass at right temporal region, polyurea and polydipsia. 1 month later, she had another mass at left frontal region.

On examination, she appeared to be sick and weak. There were soft tissue masses at right temporal and left frontal regions about 3 and 2 cm. in diameter respectively. Left periorbital swelling was noted. She did not have hepatosple-

nomegaly. Complete blood count, liver function studies were normal. Urine specific gravity test after water dehydration was 1.002.

Skull radiographs showed multiple osteolytic lesions with well-defined margins at the superolateral wall of left orbit, left frontal and right temporal bones. (Fig.2a,b) The chest radiograph was normal. There were no other bony lesions on skeletal radiographic survey. Ultrasound of abdomen showed normal findings.



2A.



2B.

**Fig.2a,b** Osteolytic lesions with well-defined margins at superolateral wall of left orbit, left frontal and right temporal bones

CT SCAN of the orbits and head without and with contrast enhancement showed an enhancing destructive soft tissue mass centered in the greater wing of left sphenoid bone,

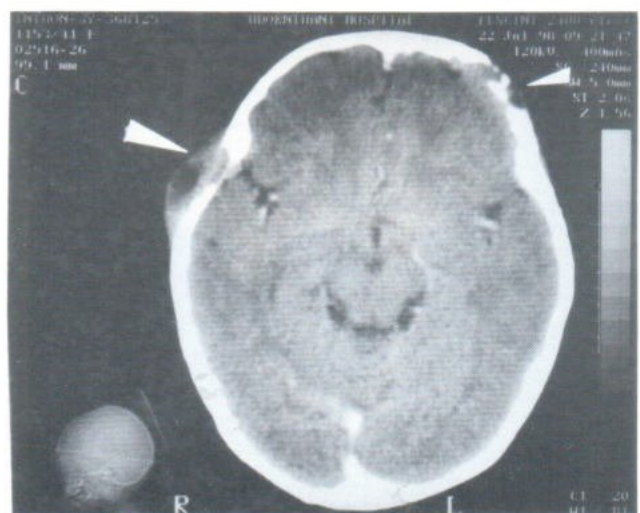
extending into the superolateral aspect of left orbit. (Fig.3) Left frontal and right temporal skull masses were noted with bony destruction. (Fig.4a,b)



**Fig.3.** Axial CECT shows enhancing soft tissue mass with bony destruction at the greater wing of left sphenoid bone, extending into the superolateral aspect of left orbit



**4A.**



**4B.**

**Fig.4a,b** Axial CECT shows left frontal and right temporal skull masses with bony destruction

The patient underwent MR imaging, on 1.5 Tesla GE Signa Horizon LX™ ( GE Medical System Milwaukee WI,USA ). Beginning with brain study, axial T1 weighted pre- and post Gadolinium (TR500 ms, TE20ms, 5.0mm.thick section, 2.0 mm. intersection spacing); Sagittal FSE T1 weighted (TR540ms, TE12.2ms, Ef) Axial FSE Proton Density weighted (TR3700ms, TE11.5ms, Ef) T2 weighted (TR3700ms, TE80.8ms, Ef ) with 5.0mm.thick section, 1.0mm.intersection spacing were done. The FOV = 12 cm., matrix size = 256 x 160 were taken.

And then pituitary fossa study was performed with coronal, sagittal pre- and post Gadolinium T1 weighted (TR400ms, TE23ms), FSE T2 weighted (TR3000ms, TE92.6,Ef).

Section thickness was 3 mm., with a gap of 0.3 mm. The FOV = 12cm., matrix size = 256x160. Flow compensation technique was used.

The study revealed an enhancing inhomogeneous iso- and hypointense mass involving the greater wing of left sphenoid bone with extension into superolateral aspect of orbital fossa causing mild exophthalmos. (Fig.5) Other cranial vault masses were noted involving inner, outer tables and diploic space at left frontal and right temporal regions. (Fig.6a,b) Areas of hyperintense on all sequence images were identified which represent subacute hemorrhage. Hypothalamus and thickness of pituitary infundibulum were normal. Absent bright spot of posterior lobe of pituitary gland was observed. (Fig.7)

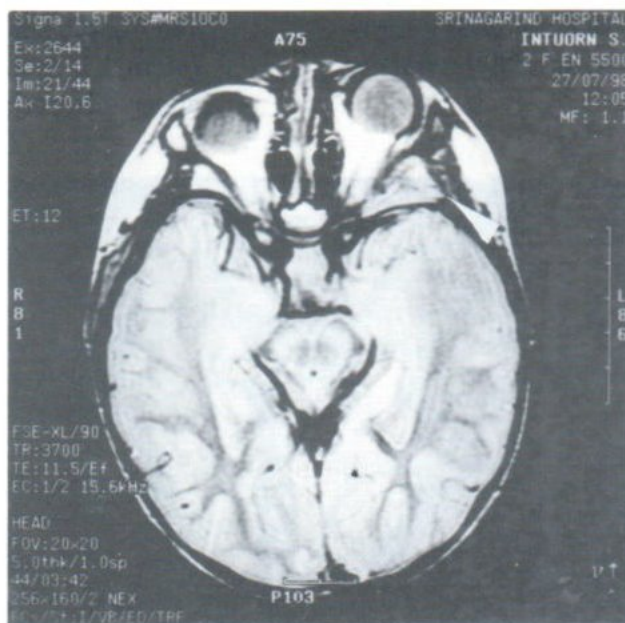


**Fig.5** Axial FSE proton density imaging shows mixed iso- and hyperintense (compare with gray matter) extraconal mass at superolateral aspect of left orbital fossa with destruction of adjacent greater wing, sphenoid bone

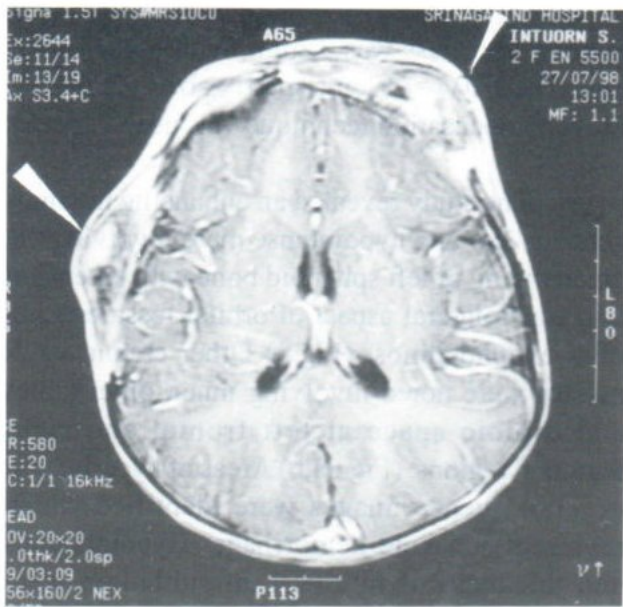


**Fig.6a** Axial SE T1W POST Gd imaging shows inhomogeneous iso-hypointense skull masses at left frontal, right temporal regions with peripheral enhancement. Internal areas of hyperintense represent bleeding foci

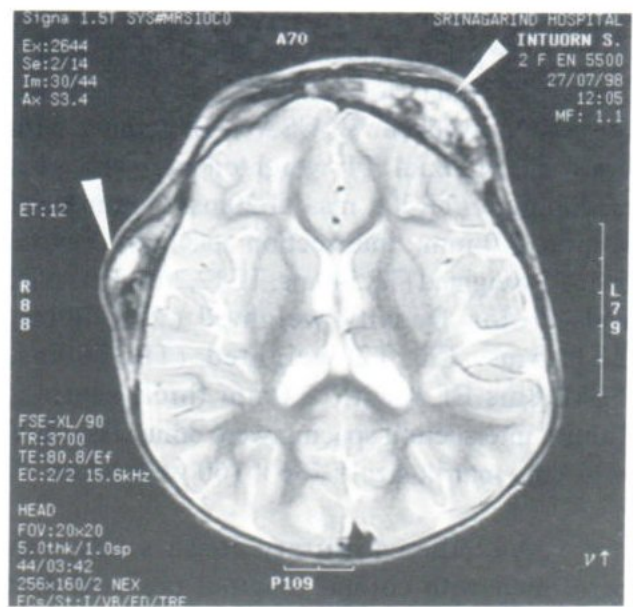


**Fig.6b** Axial FSE T2W imaging confirms these skull masses involving inner, outer tables and diploic space with abut on dura. Internal bleeding foci was visualized by areas of hyperintense

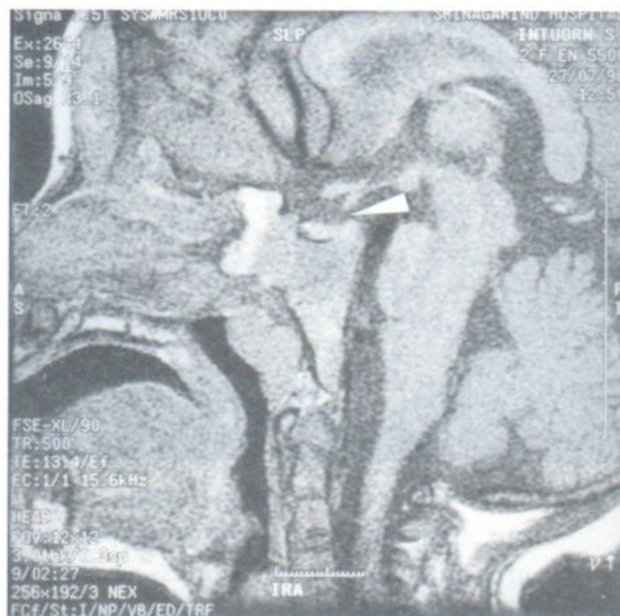


**Fig.7** Sagittal SE T1W imaging through pituitary fossa shows absence of bright spot of posterior lobe, pituitary gland. But infundibulum thickness is preserved

Left supraorbital region was incised parallel to an eye brow, disclosing an encapsulated yellowish soft tissue. (Fig.8) An excisional biopsy of left frontal mass was done. Histologic examination was diagnosis for LCH.

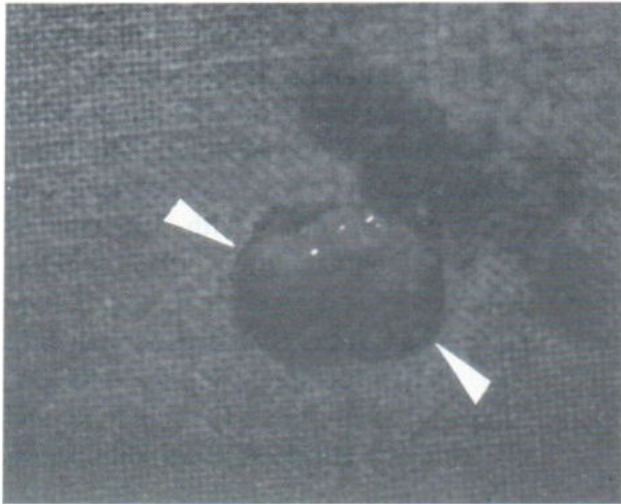


**Fig.8** Encapsulated yellowish soft tissue mass

## DISCUSSION

LCH most commonly occurs in children. It groups a spectrum of diseases in which, classically, three clinical diseases are: eosinophilic granuloma, Hand-Schuller-Christian disease and Letterer-Siwe disease. Eosinophilic granuloma is a unifocal, rarely multifocal osteolytic lesions normally limited to bone. It accounts for approximately 70% of cases of LCH.<sup>7</sup> Letterer-Siwe disease is a severe disseminated histiocytosis usually occurring below the age of 3 years with multi-organ involvement and a high mortality rate. Hand-Schuller-Christian disease is a systemic histiocytosis which the original description is the triad of exophthalmos, bony defects of the skull and Diabetes Insipidus,<sup>2,3,6,8</sup> representing 20% of all cases of LCH.<sup>7</sup> It is important to rule out disseminated disease that might occur in Letterer-

Siwe or Hand-Schuller-Christian disease, because both proper prognosis and management depend on this initial assessment and the prognosis is excellent in cases of unifocal involvement.<sup>9</sup>

The most common signs and symptoms of the orbital LCH were unilateral or bilateral proptosis, edema, erythema of the eyelid and periorbital pain. Other signs and symptoms are ptosis, optic nerve atrophy and papilledema. The lesions are usually seen in the superior or superolateral wall of the orbit.<sup>6</sup> The diagnosis should be suspected when a child or young adult presents with a short history of painful, localized swelling and radiographic evidence of bony destruction.<sup>6,9</sup> Radiographic study characteristically shows circumscribed, lytic lesions without or with surrounding sclerosis.<sup>2</sup>

CT and MR imaging scans are extremely useful to define the extent of osseous and soft tissue involvement.<sup>1,6,7,10,11</sup> On post contrast CT and MR imaging scans, lesions demonstrate moderate to marked enhancement.<sup>6,7,10</sup> MRI characteristics, usually reported, are focal lesions, surrounded by an ill-defined bone marrow and soft tissue reaction considered to represent perilesional inflammation or edema. The focal lesions are described as areas of high signal intensity in T2 weighted images and varies from low to high signal intensity on T1 weighted images.<sup>7,12,13</sup> On histological examination areas of hemorrhagic changes are seen.<sup>12,13</sup> There may be dural involvement<sup>7,14</sup> and extension into the epidural space, as well as in the temporal fossa.<sup>6</sup>

The differential diagnosis of orbital LCH from an imaging viewpoint includes rhabdomyosarcoma, juvenile fibrosarcoma, aggressive fibromatosis, lacrimal gland tumors, leukemic infiltration, granulocytic sarcoma or chloroma, metastatic neuroblastoma, metastatic Wilm's tumor and metastatic Ewing's sarcoma.<sup>2,6</sup> The diagnosis may, therefore, be in doubt until diagnosis is available.

(table 1) Orbital LCH must be differentiated from other histiocytic disorders which may involve orbit, such as sinus histiocytosis and Juvenile Xanthogranuloma (JGX). They are characterized by localized proliferation of histiocytes, but they usually confined to the orbital soft tissues and do not involve bone, although JGX may rarely result in orbital bony destruction. If there are no other systemic features, it may be difficult to distinguish between LCH and JGX clinically, but they differ in immunohistochemistry, enzymatic activity and electron microscopic features.<sup>2,6</sup>

Central nervous system involvement in LCH has been reported in 16% of the patients.<sup>15</sup> The most common intracranial sites of involvement are the hypothalamus and the pituitary.<sup>11</sup> When deposits of LCH affect the neurohypophysis (posterior lobe), diabetes insipidus may result.<sup>3</sup> On MR imaging, T1 weighted, the bright spot of posterior lobe disappears.<sup>10,16</sup>

## REFERENCES

1. Angeli SI, Alcalde J, Hoffman HT, Smith RJH: Langerhans' cell histiocytosis of the head and neck in children. *Ann Otol Rhinol Laryngol* 1995;104:173-180
2. Moore AT, Pritchard J, Taylor DSI: Histiocytosis X: an ophthalmologic review. *Br J Ophthalmol* 1985;69:7-14
3. Devaney KO, Putzi MJ, Ferlito A, Rinaldo A: Clinicopathological consultation Head and Neck Langerhans cell histiocytosis. *Ann Otol Rhinol Laryngol* 1997;106:526-532
4. Herman TE, Shackelford GD, Borders JL, Dehner LP : Unusual manifestations of Langerhans cell histiocytosis of the head and neck. *Pediatric Radiology* 1993;23:41-43
5. Stanley SS: Taking the X out of histiocytosis X. *Radiology* 1997;204:322-324
6. Hidayut AA, Mafee MF, et al: Langerhans' cell histiocytosis and juvenile xanthogranuloma of the orbit: Clinicopathologic, CT, and MR Imaging Features. *The Radiologic Clinics of North America* 1998;36:1229-1240
7. Hermans R, De Foer B, Smet MH, et al: Eosinophilic granuloma of the head and neck: CT and MRI features in three cases. *Pediatric Radiology* 1994;24:33-36
8. Cline MJ: Review article: Histiocytes and histiocytosis. *Blood* 1994;84:2840-2853
9. Glover AT, Grove AS: Eosinophilic granuloma of the orbit with spontaneous healing. *Ophthalmology* 1987;94:1008-1012
10. Bilaniuk LT, Atlas SW, Zimmerman RA: The Orbit. In: Lee SH, Rao KCGV, Zimmerman RA (eds): *Cranial MRI and CT*. McGraw-Hill, 1992, third edition, 178-179, 471
11. Kramer TR, Noecker RJ, Miller JM, et al: Langerhans cell histiocytosis with orbital involvement. *Am J Ophthalmology* 1997; 124:814-824
12. Stull MA, Kransdorf MJ, Devany KO (1992) From the archives of the AFIP: Langerhans cell histiocytosis of bone. *Radiographics* 12;801
13. Hayes CW, Conway WF, Sundaram M (1992) Misleading aggressive MR imaging appearance of some benign musculoskeletal lesions. *Radiographics* 12:1119
14. De Schepper AMA, Ramon F, Van Marck E (1993) MR imaging of eosinophilic granuloma : report of 11 cases. *Skeletal Radiology* 22:163
15. Berry DH, Becton DL. Natural history of histiocytosis X. *Hematol Oncol Clin North Am* 1987;1:23-34
16. Elster AD : Modern imaging of the pituitary. *Radiology* 1993;187:1-14